EFFECTS OF STRAIN RATE AND CO_2 ON NO FORMATION IN $CH_4/N_2/O_2$ COUNTER-FLOW DIFFUSION FLAMES

by

Fei REN, Longkai XIANG, Huaqiang CHU*, and Weiwei HAN

School of Energy and Environment, Anhui University of Technology, Ma'anshan, China

Original scientific paper
https://doi.org/10.2298/TSCI170922062R

The reduction of nitrogen oxides in the high temperature flame is the key factor affecting the oxygen-enriched combustion performance. A numerical study using an OPPDIF code with detailed chemistry mechanism GRI 3.0 was carried out to focus on the effect of strain rate (25-130 s^{-1}) and CO_2 addition (0-0.59) on the oxidizer side on NO emission in $CH_4/N_2/O_2$ counter-flow diffusion flame. The mole fraction profiles of flame structures, NO, NO_2 and some selected radicals (H, O, OH) and the sensitivity of the dominant reactions contributing to NO formation in the counter-flow diffusion flames of $CH_4/N_2/O_2$ and $CH_4/N_2/O_2/CO_2$ were obtained. The results indicated that the flame temperature and the amount of NO were reduced while the sensitivity of reactions to the prompt NO formation was gradually increased with the increasing strain rate. Furthermore, it is shown that with the increasing CO_2 concentration in oxidizer, CO_2 was directly involved in the reaction of NO consumption. The flame temperature and NO production were decreased dramatically and the mechanism of NO production was transformed from the thermal to prompt route.

Key words: *counter-flow diffusion flame, strain rate, preheated air, CO_2 addition*

Introduction

The continuous development of urbanization and industrialization leads to the increasing energy consumption and serious environmental pollution which are the threats to humanity and must be addressed. Coal, oil and natural gas, these three fossil fuels are burned emitting large amounts of pollutants such as CO_2, NO_x, SO_2, CO, and dust. What is more, a lot of CO_2 enter into the atmosphere exacerbating the *greenhouse effect*. At present, the CO_2 emissions of China have been ranked first in the world. Therefore, in order to alleviate the energy shortage and reduce pollutant emissions, it is urgent to solve the problem by burning the traditional energy in an efficient clean way [1]. It is noteworthy that the main component of natural gas, combustible ice and biogas are methane. Therefore, it is of paramount importance to study the efficient and clean combustion of CH_4. In order to further reduce the CH_4 combustion products emissions and improve fuel economy and combustion efficiency, flameless combustion technology, oxygen-rich combustion technology and flue gas recycling and other combustion technologies have been used for efficient clean combustion of CH_4.

With the continuous enrichment of experimental methods and the deepening application of numerical simulation in combustion research, related scholars have done a lot of research on opposed-jet diffusion flame [2-5]. Although the previous studies manifests sub-

* Corresponding author, e-mail: hqchust@163.com

stantial efforts have been done on the CH_4 opposed diffusion flame, there is still relatively less to systematically change the operating conditions to further understand its influence on CH_4 counter-flow diffusion flame. It is beneficial to simplify NO mechanism and deepen understanding NO formation in high temperature flue gas circulation technology.

The aim of this study is to explore numerically the effect of strain rate (25-130 s^{-1}) and CO_2 addition (0-0.59) on the oxidizer side on NO emission in $CH_4/N_2/O_2$ counter-flow diffusion flame at atmospheric pressure using an OPPDIF code [6] with detailed chemistry mechanism GRI 3.0 [7]. The combustion temperature and the mole fraction of NO, NO_2 and some selected radicals (H, O, OH) distribution profiles and the sensitivity of the dominant reactions contributing to NO formation in the flames of $CH_4/N_2/O_2$ and $CH_4/N_2/O_2/CO_2$ were obtained.

Model and mechanism

The counter-flow diffusion flame model is formed by two coaxially opposing nozzles, one jet of the fuel and the other of the air-flow. In this paper, the fuel jet is located at an axial position of 0 cm and the oxidizer is located at 2.0 cm, giving a separation distance of two nozzles of 2.0 cm. The flame surface and the stagnation plane will be formed in the two nozzles. The model can be approximated as 1-D combustion, the schematic drawing of counter-flow diffusion flame shown in fig. 1. The jet flow velocity of the reactants are determined by the strain rate, which has a critical effect on the ignition and extinction of the counter-flow diffusion flame and has a certain effect on combustion temperature, the flame thickness and the pollutant generation (NO_x, CO) [8]. The symbol of the strain rate is defined as κ via the following relationship formula:

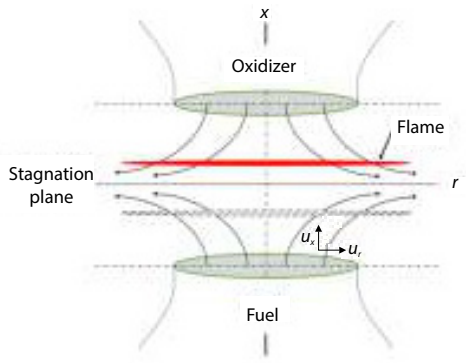

Figure 1. Schematic of a counter-flow diffusion flame

$$\kappa = 2\frac{V_O}{L}\left(1+\frac{V_F}{V_O}\sqrt{\frac{\rho_F}{\rho_O}}\right) \tag{1}$$

$$\rho_F V_F^2 = \rho_O V_O^2 \tag{2}$$

where V_O and V_F are the oxidizer and fuel exit velocities, respectively, L – the nozzle gap of 2.0 cm, and ρ_O and ρ_F are the density of oxidizer and fuel, respectively.

According to previous experimental and numerical survey [8-12], GRI 3.0 mechanism (contained 53 kinds of species and 325 elemental reactions) was selected in present work. Before the calculation was carried out, the cases in [9] were calculated repeatedly, finding the results are in a good agreement. In this study, the fuel-flow was pure CH_4 whose temperature was always at 300 K and the oxidizer side was $N_2/O_2/CO_2$. Three specific simulation conditions are shown in tab. 1.

Table 1. Simulation cases

Case	Strain rate, κ [s^{-1}]	Oxidizer temperature [K]	Oxidizer		
			N_2	O_2	CO_2
A	25-130	300	0.79	0.21	0
B	100	1200	0.2	0.80-0.21	0-0.59

Results and discussion

The effect of different strain rates

The strain rate can largely affect the flame structure (the mole fraction of species and temperature distribution cross the flame) [8]. Figure 2 shows the flame structures in case A at four strain rates (25 s^{-1}, 60 s^{-1}, 100 s^{-1}, and 130 s^{-1})**.** When the strain rate increases, the mole fraction of CO_2 and H_2O are reduced and the peak temperature of the flames are 2071.379 K, 2039.546 K, 2012.934 K, and 1996.368 K, respectively. It can be seen that the peak flame temperature decreases with the increase of the strain rate and the peak temperature drop is 75 K. According to the approximate relationship between the strain rate and the thickness of the flame: $\delta \sim (D/\kappa)^{1/2}$ [3], when the diffusion rate, D, is specific, the flame thickness (reaction region) gradually decreases and the reaction zone shrinks closer to the fuel side as the strain rate increases.

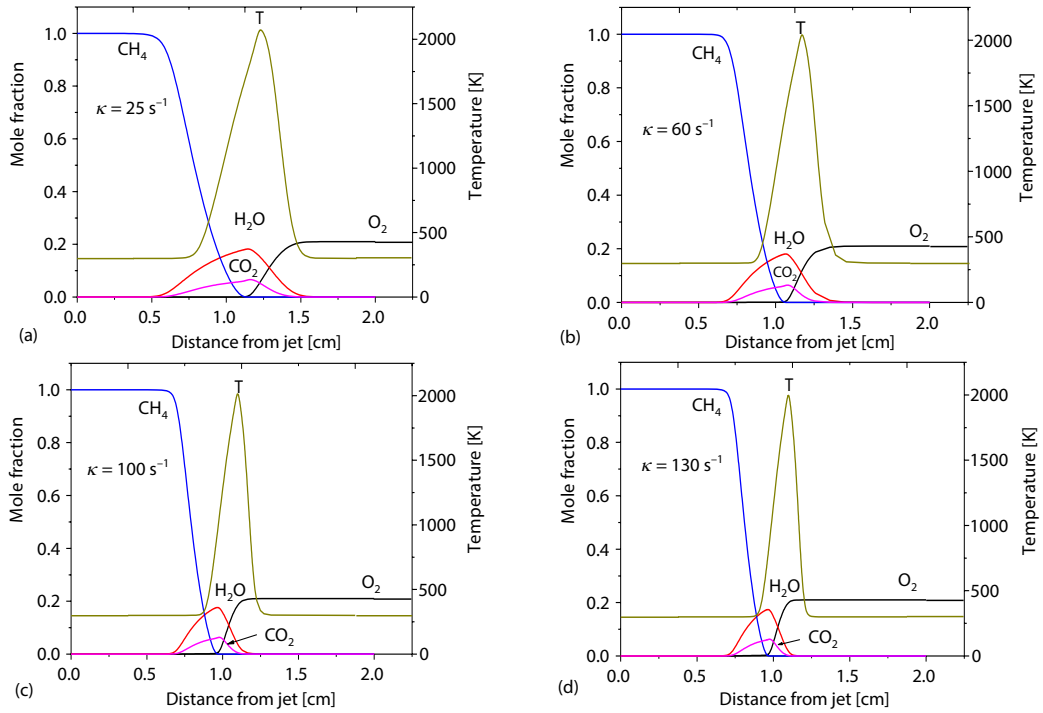

Figure 2. Flame structures profiles for different strain rates

Sahu *et al*. [13] concluded that the concentration of three radicals, O, H, and OH, plays an important role in the heat release and the flame combustion temperature. Figure 3 shows the change in the peak mole fraction of three radicals with respect to the strain rate. It can be seen from fig. 3, with the increasing strain rate, the OH peak concentration slightly decreased while H, O peak generation increased. The increasing strain rate directly reduces residence time in the combustion reaction zone, which leads to incomplete combustion hence the peak flame temperature is decreased. As NO and NO_2 production occupy a large proportion in the combustion pollutants, the maximum temperature and NO_x peak values varied with different strain rates are shown in fig. 4. In fig. 4, both the peak flame temperature and NO_x peak mole fraction are decreased with the increase of the strain rate. They are positively correlated, but have a

negative correlation to strain rate. Figure 5 shows the mole fraction of NO and NO_2 at different strain rates. It can be seen that the NO and NO_2 formation regions move gradually toward the fuel side with the increase of the strain rate, and as the strain rate increases from 25 s^{-1} to 130 s^{-1}, the two concentrations decrease by more than 50%. Compared to NO_2, NO has only one peak value produced more close to the fuel side. The mole fraction of NO_2 has two peak values, which one appears in the vicinity of fuel side and the second peak appears near the oxidant side. The NO_2 is affected by the reductive atmosphere, and the amount of CO produced at the center of two nozzles is relatively large so that at the center, the concentration of NO_2 produced is the highest. The NO concentration is two orders of magnitude larger than NO_2. To further analyze the mechanism of NO_x formation, a sensitivity analysis of NO was conducted.

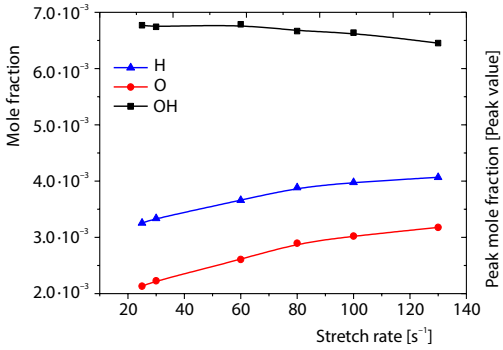

Figure 3. The H, O, and OH peak mole and fraction for different strain rates

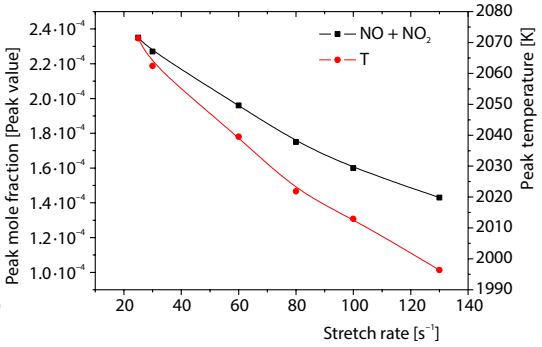

Figure 4. The maximum temperature NO_x peak values for different strain rates

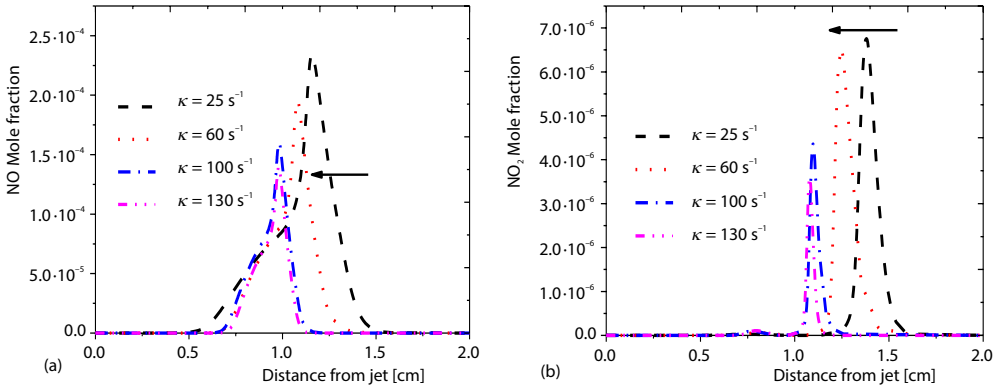

Figure 5. The mole fraction of NO and NO_2 for different strain rates

There are two main theories about NO_x formation: Zeldovich routine (thermal NO_x) and Fenimore theory (prompt NO_x). Thermal routine is nitrogen molecules directly involved in the reaction at high temperature oxidized to NO_x and the main source of NO is produced in high temperature combustion. The prompt NO_x formation is due to the decomposition of hydrocarbons into various small hydrocarbon groups during combustion then the small hydrocarbon groups react with nitrogen molecules to form amine and cyano radials producing NO. Other specific NO formation routine are N_2O, NNH, and NO re-burning routines. The NO re-burning mechanism is mainly that NO is reduced to HCN or HCNO by reacting with CH, CH_2 and CH_3, or further oxidized to NO_2 [14, 15].

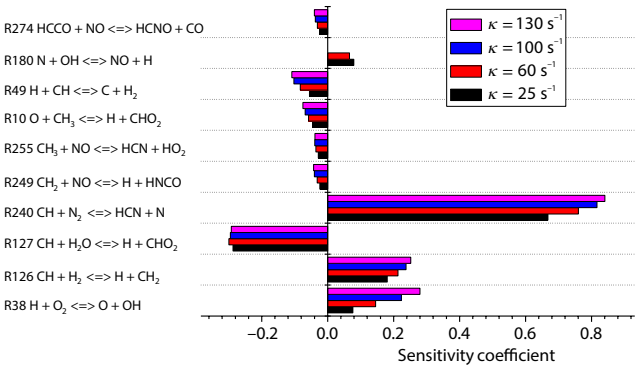

Figure 6. Sensitivity analyses for different strain rates

Figure 6 shows the sensitivity of the dominant reactions contributing to NO formation at the peak temperature position for different strain rates. As can be seen, the reaction with the greatest influence on the NO formation at low strain rate is R240 CH + N_2 <=> HCN + N. This reaction is a step in the prompt routine, indicating that the prompt NO has the dominant in the NO_x. The R126 CH+H_2<=>H+CH and R38 H + O_2 <=> O + OH are also important in producing NO and with the increasing strain rate, the effect of the three reactions gradually reduced. The main reaction to NO consumption is R127 CH + H_2O <=> H + CH_2O and this reaction consumes CH to suppress the progress of R240, and the formation of H promotes the R38. It should be noted that R38 can be as the main heat consumption reaction [10, 16]. The R255 CH_3 + NO <=> HCN + H_2O and R249 CH_2 + NO <=> H + HNCO belong to the NO re-burning reactions and promote the consumption of NO as the strain rate increasing. Therefore, with the increased strain rate, the flame temperature is decreased and the reactions to prompt NO are enhanced, but the consumption of NO is larger than its production, leading to the decrease in NO formation.

Effect of CO_2 addition on the oxidizer side

A certain amount of CO_2 addition to the hydrocarbon fuel has a significant effect on the flame structure. The CO_2 has the heat and mass transfer in the combustion process. Thus, the effects of CO_2 addition on the fuels in combustion have been studied in recent years [1, 4, 5, 8, 11, 17]. For this reason, the initial temperature of the fuel side is set to 300 K and the oxidant flow is 1200 K. The strain rate is kept at 100 s^{-1} and the oxidant side is oxygen-enriched O_2/N_2 (0.8/0.2) CO_2 (0.1-0.59) (for convenience, molar fraction replaced by volume fraction). Figure 7 gives flame structure profiles for CO_2 addition.

It can be seen that the positions of A, B, C, and D in fig. 7 are the distance from the fuel side where CH_4 starts to consume. That $X_A < X_B < X_C < X_D$ shows that with the increase of CO_2 concentration, the consumed position of CH_4 move to the oxidizer side. The peak flame temperature decreases gradually when the CO_2 concentration increases from 0.1 to 0.59 (relatively, O_2 concentration decreases from 0.8 to 0.21), and the peak temperature decreases by 802 K. Further observation, with the increasing CO_2 addition, the combustion reaction area become smaller and is closer to the high temperature oxidant side. This is mainly due to the constant oxidizer flow velocity, the reduction of O_2 concentration and the dilution, the thermal and the chemical effect of CO_2. With the increasing CO_2 concentration, the amount of H_2O is gradually decreased.

Figure 8 shows the mole fraction of H, O, and OH concentration at different preheating temperatures. It can be seen that when the CO_2 concentration increases, the peak OH mole fraction decreases to 1/10, and the peak values of H and O decrease to 1/15. The peak flame temperature and the mole fraction of OH, O, and H are negatively correlated with CO_2 concentration. Figure 9 shows the peak temperature and peak NO_x mole fraction of the flame at different preheating temperatures. From fig. 9, it can be obtained that when the CO_2 concentration increases, the peak flame temperature has parabolic changes and gradually reduced. The peak val-

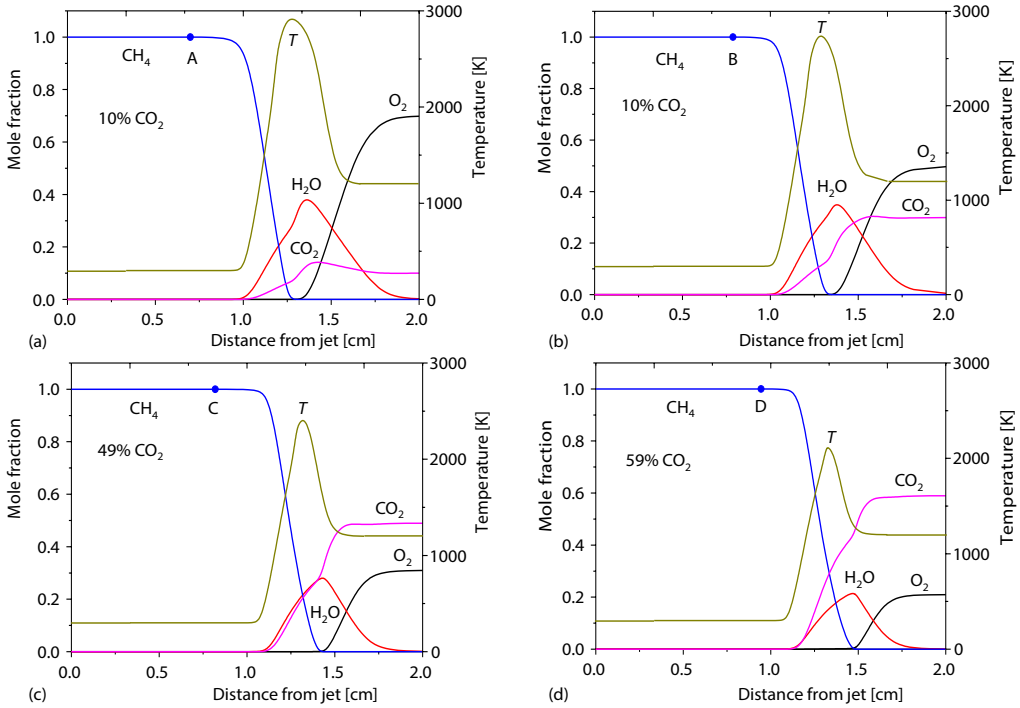

Figure 7. Flame structure profiles for CO_2 addition

ue of NO_x formation is exponentially decreased with the increasing CO_2 concentration due to the decreasing reaction temperature affecting the NO_x formation. Figure 10 gives the mole fraction of NO and NO_2 at different CO_2 concentrations. With the increasing CO_2 concentration, the NO and NO_2 formation regions gradually move toward the oxidizer side. In addition, when CO_2 addition is increased from 0.1 to 0.59, the NO and NO_2 concentrations are significantly decreased.

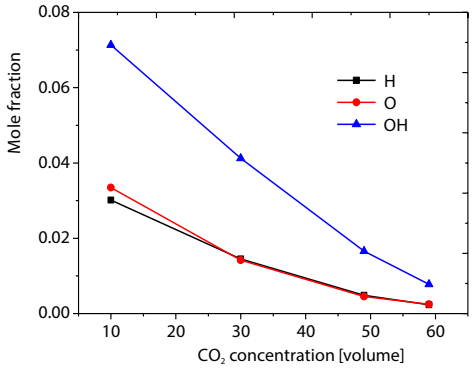

Figure 8. The H, O, and OH peak mole fraction for CO_2 addition

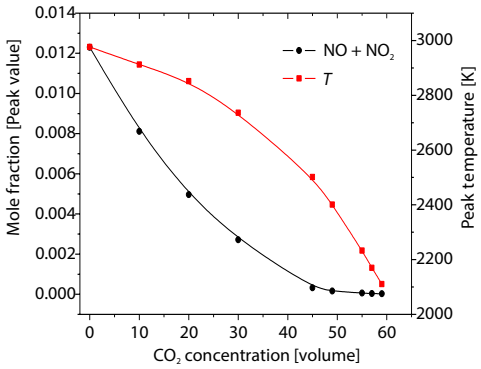

Figure 9. The maximum temperature and NO_x peak values for CO_2 addition

Figure 11 shows the sensitivity of the dominant reactions contributing to NO formation at different CO_2 concentrations. When the oxidant side is without CO_2 addition, R178 N + NO <=> N_2 + O dominate NO formation, and the sensitivity of R178 to NO increases first and then decreases with the increasing CO_2 concentration. Furthermore, the sensitivity of R178

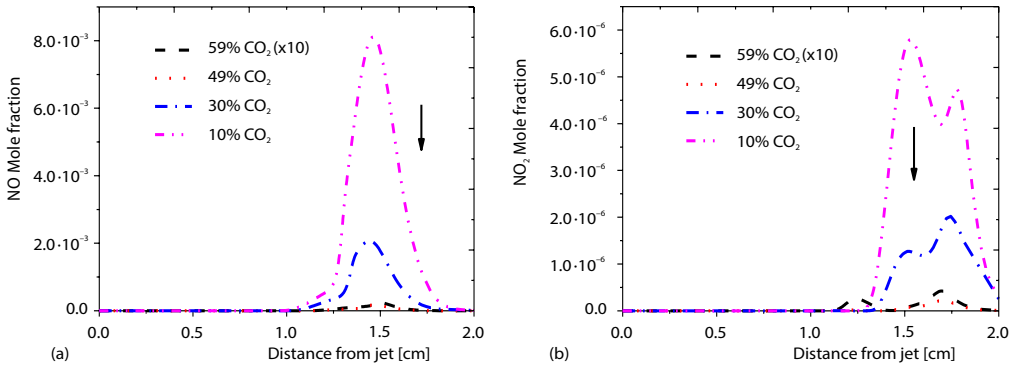

Figure 10. The mole fraction of NO and NO_2 for CO_2 addition

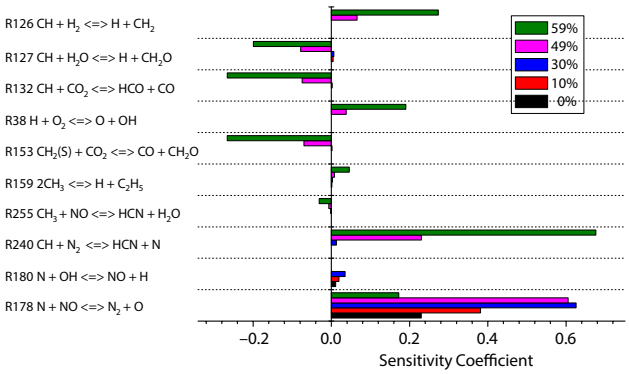

Figure 11. Sensitivity analyses for CO_2 addition

to NO formation is the highest when CO_2 adding concentration is 0.3. The effect of R240 CH + N_2 <=> HCN + N on the NO formation is gradually higher than that of R178, which is mainly due to the decreasing temperature. The R126 CH + H_2 <=> H + CH_2 and R38 H + O_2 <=> O + OH also have a great influence on NO production. When the CO_2 concentration increases, R127 CH + H_2O <=> H + CH_2O turn to suppress the NO formation dominated by R240. The suppression effect of R132 CH + CO_2<=>HCO + CO and R153 CH_2(S) + CO_2<=> CO + CH_2O on NO formation is obviously related to CO_2 concentration. The CO_2 is involved in the consuming reactions of CH and CH_2(S). Therefore, with the CO_2 addition to the oxidizer side in a high temperature, the main NO formation routine was changed from thermal to prompt and can effectively reduce the thermal NO formation.

Conclusions

Based on the OPPDIF model with detailed chemistry mechanism GRI 3.0, the effects of strain rate, preheated temperature and CO_2 addition on the oxidizer side on the flame temperature, O, H, OH, and NO mole fraction were investigated by simulating the 1-D counter-flow diffusion flames. Moreover, the sensitivity analysis of the main reactions to NO formation was conducted. The main conclusions were as follows.

- At low strain rate, as the strain rate increasing, the flame temperature was decreased, resulting in a decrease in NO formation and combustion reaction zone moving toward the fuel side. In addition, the sensitivity of the prompt NO routine gradually increased.
- Under the condition of oxygen enrichment, as CO_2 concentration in O_2/N_2 increasing, relatively, the concentration of O_2 decreasing, the flame temperature decreased gradually and the combustion reaction area moved to the oxidizer side. Furthermore, the main NO formation routine was changed from thermal to prompt one and the reaction of NO consumption was improved. The CO_2 is directly involved in the reaction of NO consumption.

Acknowledgment

The authors would like to thank National Key R&D Program of China (Grant No. 2017YFB0601805) and the National Natural Science Foundation of China (Grant No. 51676002) for their financial support of this study.

Nomenclature

D – the finite diffusion rate, [cm^2s^{-1}]
L – the nozzle gap, [cm]
V_O, V_F – the oxidizer exit velocity and fuel exit velocity, [cms^{-1}]
u_x, u_r – the velocity in x-direction and radial direction, [cms^{-1}]

Greek symbols

δ – the flame thickness, [cm]
κ – the strain rate, [s^{-1}]
ρ_O, ρ_F – the oxidizer density and the fuel density, [gcm^{-1}]

References

[1] Gu, M., *et al*., Effects of Simultaneous Hydrogen Enrichment and Carbon Dioxide Dilution of Fuel on Soot Formation in an Axisymmetric Coflow Laminar Ethylene/Air Diffusion Flame, *Journal Combustion & Flame*, *166* (2016), Feb., pp. 216-228
[2] Thomsen, D. D., Laurendeau, N. M., Lif Measurements and Modeling of Nitric Oxide Concentration in Atmospheric Counterflow Premixed Flames, *Combustion & Flame*, *124* (2001), 3, pp. 350-369
[3] Sung, C. J., *et al*., Structural Response of Counterflow Diffusion Flames to Strain Rate Variations, *Combustion & Flame*, *102* (1995), 4, pp. 481-492
[4] Park, O., Fisher, E. M., Effect of Oxycombustion Diluents on the Extinction of Nonpremixed Methane Opposed-jet Flames, *Combustion Science and Technology*, *188* (2016), 3, pp. 370-388
[5] Gascoin, N., *et al*., Thermal Effects of CO_2 on the NO_x Formation Behavior in the CH_4 Diffusion Combustion System, *Applied Thermal Engineering*, *110* (2016), Jan., pp. 144-149
[6] Kee, R. J., *et al*., A Fortran Program for Modelling Steady Laminar One Dimensional Premixed Flames, Report No. SAND85-8240, Sandia National Laboratories, Albuquerque, N. Mex., USA,1985
[7] Smith, G. P., *et al*., GRI-MECH 3.0, http://www.me.berkeley.edu/gri_mech/
[8] Liu, F., *et al*., The Chemical Effect of CO_2, Replacement of N_2, in Air on the Burning Velocity of CH_4 and H_2 Premixed Flames, *Combustion & Flame*, *133* (2003), 4, pp. 495-497
[9] Cheng, Z. X., *et al*., Experimental and Numerical Studies of Opposed-Jet Oxygen-Enhanced Methane Diffusion Flames, *Combustion Science and Technology*, *178* (2006), 12, pp. 2145-2163
[10] Zou, C., *et al.*, The Chemical Mechanism of Steam's Effect on the Temperature in Methane Oxy-Steam Combustion, *International Journal of Heat & Mass Transfer*, *75* (2014), Aug., pp. 12-18
[11] Kim, S. G., *et al*., Thermal and Chemical Contributions of Added H_2O and CO_2 to Major Flame Structures and NO Emission Characteristics in H_2/N_2 Laminar Diffusion Flame, *International Journal of Energy Research*, *26* (2002), 12, pp. 1073-1086
[12] Seiser, R., Seshadri, K., The Influence of Water on Extinction and Ignition of Hydrogen and Methane Flames, *Proceedings of the Combustion Institute*, *30* (2005), 1, pp. 407-414
[13] Sahu, A. B., *et al*., Quantitative OH Measurements and Numerical Investigation of H_2/CO Kinetics in Syngas-Air Counterflow Diffusion Flames, *Fuel*, *193* (2017), Apr., pp. 119-133
[14] Mendiara, T., Glarborg, P., Reburn Chemistry in Oxy-Fuel Combustion of Methane, *Energy & Fuels*, *23* (2009), 7, pp. 3565-3572
[15] Normann, F., *et al.*, Reburning in Oxy-Fuel Combustion: A Parametric Study of the Combustion Chemistry, *Industrial & Engineering Chemistry Research*, *49* (2010), 19, pp. 9088-9094
[16] Nikolaou, Z. M., Swaminathan, N., Heat Release Rate Markers for Premixed Combustion, *Combustion & Flame*, *161* (2014), 12, pp. 3073-3084
[17] Chu, H., *et al.*, A Comprehensive Evaluation of the Non-Gray Gas Thermal Radiation Using the Line-by-Line Model in One- and Two-Dimensional Enclosures, *Applied Thermal Engineering*, *124* (2017), Sept., pp. 362-370

Paper submitted: September 22, 2017
Paper revised: December 28, 2017
Paper accepted: December 30, 2017